Desalination and Water Treatment
www.deswater.com
doi: 10.5004/dwt.2022.28448

264 (2022) 205–214
July

Ni–Fe and Zn–Fe LDHs synthesized by co-precipitation method at variable pH: application to the removal of Cochineal Red A dye from aqueous solution

Rachida Mendil*, Noureddine Nasrallah

Laboratory of Reaction Engineering, Faculty of Mecanical Engineering and Process Engineering, University of Sciences and Technology Houari Boumediene (U.S.T.H.B) 16000, Algiers, Algeria, emails: rachmend84@hotmail.com (R. Mendil), nas_nour@yahoo.fr (N. Nasrallah)

Received 20 June 2021; Accepted 14 February 2022

ABSTRACT

Co-precipitation at constant pH is a common method for the preparation of layered double hydroxides (LDHs) and related materials. In this work, Ni–Fe and Zn–Fe materials were co-precipitated at variable pH and characterized by X-ray diffraction and infrared spectroscopy. The batch method for evaluating the adsorption of Cochineal Red A dye into prepared materials was investigated. It has found that the sorbed amount depends on the nature and content of bi- and trivalent metal ions in LDH. The removal of Cochineal Red A dye reaches its maximum of 98.44% and 96.86% after 60 and 80 min for Ni–Fe and Zn–Fe respectively with the use of the optimum masses of 40 and 100 mg for these respective materials. Freundlich and Temkin isotherm models were applied to describe the equilibrium sorption experimental data. The Cochineal Red A dye sorption follows the Temkin model with high coefficient correlation for the two materials. This indicates that the adsorption is characterized by a uniform distribution of binding energies between the molecules adsorbed and adsorbents. The sorption kinetics data fitted the pseudo-second-order model. Adsorption experiments were carried out as a function of pH, temperature and sorbent dose. The sorption was found to be a pH independent for Ni–Fe material, whereas, higher pH potentially causes dissolution of Zn–Fe material. Thermodynamic study indicates that the sorption process is spontaneous and endothermic in nature.

Keywords: Cochineal Red A; Layered double hydroxide; Adsorption; Kinetic

1. Introduction

Organic dyes are widely used in textile, leather, cosmetic, plastic, paper, food, petroleum and some other industries such as nylon, wool, silk and inkjet printing [1–3].

Due to significant growth of this class of industries, the increase of discharge of dye wastewater has been recorded over the past years [4].

Many organic dyes have a harmful effect on human health (dysfunction of kidneys, reproductive system, liver, brain and central nervous system) and are characterized as carcinogenic [5].

Cochineal Red A, azo dye is largely used in different industrial fields including food, cosmetics, drugs, textile and pharmaceutical industries [6–8].

Several diseases such as occupational asthma, anaphylaxis, urticarial, angioedema, bronchospasm or aggravation of atopic dermatitis and food allergy known to be caused by this dye have been reported. It may increase hyperactivity in affected children and adversely affect those that are sensitive to aspirin [9–12].

* Corresponding author.

Due to its toxic and carcinogenic effects, it needs to be removed before the wastewater can be discharged.

Dyes and colorants contaminants are removed by many techniques such as chemical degradation, biological degradation, photochemical degradation, electro-coagulation, sedimentation, adsorption, membrane process and the combined treatment of different methods. Electrocoagulation is an efficient and cost-effective method for removing organic pollutants. Also electrocoagulation is found to be more effective than advanced oxidation process (e.g., UV/TiO_2) for removal of organic compounds in terms of efficiency and electrical energy consumption. [13–18].

Adsorption is one of the best wastewater treatment method. It has several advantages such as operating flexibility, high removal efficiency on a wide range of substances, possibility to recycle many adsorbents and insensibility to toxicants [2,19,20].

Activated carbon, bentonite, and metal oxides, fly ash and coal are widely used to remove dyes from aqueous solutions [21]. However, there are certain drawbacks associated with these adsorbent materials, such as relatively low adsorption capacity, difficulty to reuse, high preparation cost, unstable properties and secondary pollution. Therefore, the research has been focused on developing adsorbents with higher affinity, capacity and selectivity for the target pollutants. Layered double hydroxides (LDHs) which have moderate chemical stability, low cost and non-toxicity are also known as hydrotalcite-like materials or anionic clays, are represented by the general formula $[M^{2+}_{1-x}M^{3+}_{x}(OH)_2][A^{m-}_{x/m}, nH_2O]$, where M^{2+} is a divalent metal cation such as Mg^{2+}, Zn^{2+} and Cu^{2+}, M^{3+} is a trivalent metal cation such as Al^{3+}, Fe^{3+} and Cr^{3+}, A^{m-} is the exchangeable interlayer anion and x is defined as the ratio between divalent and trivalent cations with different values between 0.2 and 0.33 [22]. LDH is an attractive adsorbent candidate for selectively removal of anionic dye pollutants [16,23–25]. For instance, Lafi et al. studied the adsorption for Congo red using Mg–Al LDH, and it was found that the maximum adsorption capacity was 111.11 mg/g. Ahmed et al. synthesized Mg–Fe LDH for the extraction of Congo red from aqueous solution, and the maximum adsorption capacity was found to be 104.6 mg/g. Recently, LDH based nano-composites such as those hybridized with carbon materials, polymers or anions have been increasingly studied for the removal of various toxic pollutants from aqueous solutions. For example, Yang et al. studied the adsorption efficiency of Congo red on CNT/MgAlO and revealed significant improvement in surface area after CNT hybridization which increased the adsorption capacity of dye. Similarly, Zhang et al. investigated the adsorption performance of methylene blue on carbon dot/Mg–Al LDH and demonstrated that the presence of C-dots in LDH improved the removal efficiency due to the reaction of methylene blue with surface hydroxyl groups in the C-dots [21,26,27]. Several methods, such as co-precipitation at constant pH, hydrothermal, ion exchange, and sol–gel have been used to synthesize LDH in the laboratory [26]. However, the study on the application of LDH synthesized by co-precipitation at variable pH as adsorbent for dyes removal is rarely reported. The objectives of the present study were to synthesize two different materials Ni–Fe and Zn–Fe by co-precipitation method at variable pH and to evaluate the sorption performance of the prepared materials for their capacity to remove acid dye Cochineal Red A from water.

From the literature, no information for the Cochineal Red A removal by the synthesized materials in the present work is available. The relevant parameters such as adsorbent dosage, solution pH, contact time and temperature were optimized for the best adsorption performance of prepared materials. Adsorption kinetics, isotherms and thermodynamics were used to expound the specific adsorption mechanism. The regeneration of the adsorbent was examined to verify the reusability of materials.

2. Experimental

2.1. Materials

Iron(III) chloride hexahydrate, $FeCl_3{\cdot}6H_2O$ (from Alfa Aesar, 97%, Port of Heysham Industrial Park Heysham, Lancashire LA3 2XY United Kingdom), chloride acid 0.1 N, HCl (from Biochem, 37%–38%, BP 3496, Lome, Togo), zinc chloride, $ZnCl_2$ (≥98%), nickel(II) chloride, $NiCl_2$ (98%), sodium hydroxide 2 M, NaOH (99.8%) and acetone (≥99.5%) are from Sigma-Aldrich (3050 Spruce St. Louis Missouri, 63103 United States) and are used as received.

2.2. Sorbents synthesis

Ni–Fe and Zn–Fe LDHs were synthesized through a co-precipitation method at variable pH with [Ni]/[Fe] and [Zn]/[Fe] ratio equal to 2 as described by Fernando Pereira de Sá et al. [28].

The Zn–Fe LDH was prepared in a solution containing 0.14 mol of $Zn(Cl)_2$, 0.07 mol of $Fe(Cl)_3{\cdot}6H_2O$ and 100 mL of distilled water. This solution was slowly added to a solution containing 200 mL of NaOH (2 M) while moderately agitation until a pH between 7 and 9. The obtained precipitate was washed, dried at 70°C overnight and then grounded into fine powder by an agate mortar.

A Ni^{2+}/Fe^{3+} LDH chloride was prepared by a method analogous to the Zn–Fe LDH described above, except that $Ni(Cl)_2{\cdot}6H_2O$ (20 g) and $Fe(Cl)_3{\cdot}6H_2O$ (11.37 g) were used as the source of nickel and iron and the pH was between 9 and 10.

2.3. Sorbate

Fig. 1 shows the molecular structure of Cochineal Red ($C_{20}H_{11}N_2Na_3O_{10}S_3$) which is an acid and azoic dye [29].

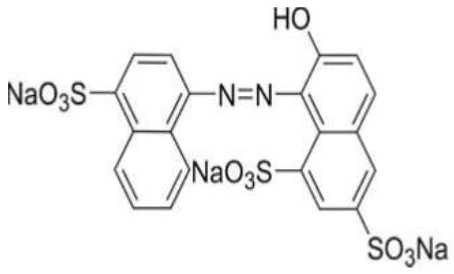

Fig. 1. Cochineal Red A structure.

2.4. Characterization of the prepared materials

Powder X-ray diffraction data were collected with CuK_α radiation (λ = 1.54056) using a Philips X'PERT-PRO diffractometer (Maryland Hall 45). The IR spectra of the synthesized materials were performed with an Alpha Bruker FTIR spectrometer (Rudolf-Plank-Str. 27 Ettlingen 76275 Germany) over the 4,000–400 cm^{-1} wavenumber range.

3. Study of Cochineal Red removal with synthesized materials

3.1. Kinetic study

For kinetic studies, a suspension was prepared by the addition of 400 mg of prepared materials in 250 mL of different Cochineal Red A dye solutions. Experiments were carried out at room temperature and at constant stirring (500 rpm). After selected time intervals, 5.0 mL of the samples were stirred then centrifuged. The dye concentration was determined at 507 nm by UV-Visible spectrophotometer (OPTIZEN 3220UV).

The initial concentration of Cochineal Red A dye were ranged from 10 to 70 mg/L.

The quantity of dye adsorbed at time t was calculated by using the following equation:

$$q_t = \frac{(C_i - C_t)V}{m} \quad (1)$$

where C_i (mg/L) is the initial concentration of the Cochineal Red A dye solution, C_t is the concentration of Cochineal Red A dye present at time t (mg/L), V is the volume of the solution (L) and m is the mass of adsorbent (g).

3.2. Sorption isotherms

The sorption isotherms for each system of materials/adsorbate were studied by adding 80 mg of materials suspensions with Cochineal Red A in aqueous solution. 50 mL of dye solution ranging from 10 to 70 mg/L were shaken for 2 h at room temperature then centrifuged. The dye equilibrium concentration was determined by visible spectrophotometer at 507 nm.

The quantity of dye adsorbed at equilibrium was calculated by the following expression:

$$q_e = \frac{(C_i - C_e)V}{m} \quad (2)$$

where C_i (mg/L) is the initial concentration of Congo red (CR) solution, C_e is the concentration of CR present at equilibrium (mg/L), V is the volume of the solution (L), m is the mass of adsorbent (g) and q_e is the quantity of sorbate adsorbed at equilibrium (mg of dye per g of sorbent).

3.3. Temperature effect

This effect was studied at four constant temperatures (298, 308, 318 and 328 K), fixed initial dye concentration (C_i) of 50 mg/L and sorbent mass of 80 mg. The solutions were stirred for 2 h then centrifuged. The quantities of sorbate adsorbed at equilibrium were determined as above.

3.4. pH initial effect

The effect of pH initial on the removal of dye by synthesized materials was carried out at pH ranging from 2 to 11, fixed initial dye concentration (C_i) of 50 mg/L and sorbent mass of 80 mg. The solutions were stirred for 2 h then centrifuged. The dye concentration is determined as above.

3.5. Sorbent dosage effect

This effect was studied on suspension of materials in 50 mg/L of dye solution by varying sorbent quantities from 20 to 200 mg at natural pH of the solution dye. The suspensions were stirred for 2 h then centrifuged. The quantities of sorbate adsorbed at equilibrium were determined as above.

3.6. Adsorbent regeneration and recyclability

The possibility of regeneration is an important factor for the evaluation of the adsorbent. In order to study the recyclability of the adsorbents, the desorption experiments of Cochineal Red dye were performed by acetone extraction of the sorbed dye followed by drying of the solids at 40°C overnight [30]. The resulting materials were used to remove dye from aqueous solutions at the same solid/solution ratio as in the sorption study (a solid/solution ratio of 1.75 g/L and an initial concentration of 30 mg/L).

4. Results and discussion

4.1. Characterization of materials

X-ray diffraction patterns of synthesized materials are shown in Fig. 2.

The peaks of Ni–Fe LDH located at (003), (006), (012), (110) and (113) are attributed to the characteristics peaks of LDH.

The X-ray diffraction (XRD) pattern shows peaks of NaCl at 27.39° (111), 31.69° (200), 45.35° (220), 53.98° (311), 56.60° (222), 66.27° (400) and 75.35° (420), in good agreement with the reference pattern of NaCl (00-001-0993) which can be attributed to the reaction of Na^+ with Cl^-.

The pattern shows peaks at 33.85° and 44.85° associated to either $Ni(OH)_2$ or $Fe(OH)_3$. Because the as-synthesized Ni–Fe exhibits poor crystalline structure, the lower diffraction intensity was observed [31].

The XRD patterns of the Zn–Fe show that no hydrotalcite structure is formed under the synthesis conditions used. It is composed of one major crystalline phase identified as ZnO due to the synthesis conditions used; based on Zn solubility curves, precipitation of ZnO starts at pH 9 [32].

Infrared spectra of the synthesized materials shown in Fig. 3 indicate bands characteristics of layered double hydroxide compounds. The broad bands observed at 3,352 cm^{-1} for both spectra are attributed to the stretching mode of hydrogen-bonded hydroxyl groups from both the hydroxide layers and interlayer water [33]. The bands around 1,632 as shown in Fig. 3 represent H–O–H bending vibration of water [34,35]. While the bands recorded at 1,352 and 1,362 cm^{-1} can be attributed to the carbonate ions, which might have been formed by the adsorption of atmospheric CO_2 [30].

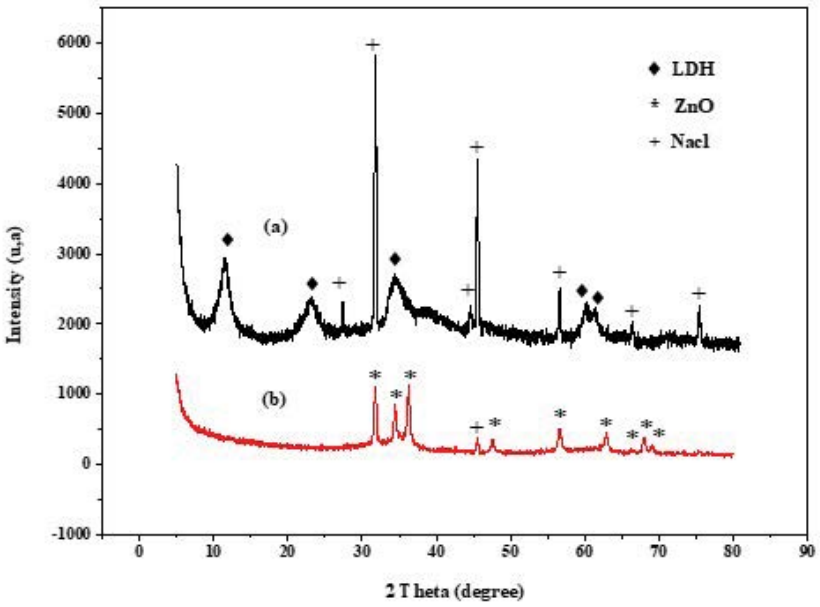

Fig. 2. XRD patterns of synthesized (a) Ni–Fe and (b) Zn–Fe LDHs samples.

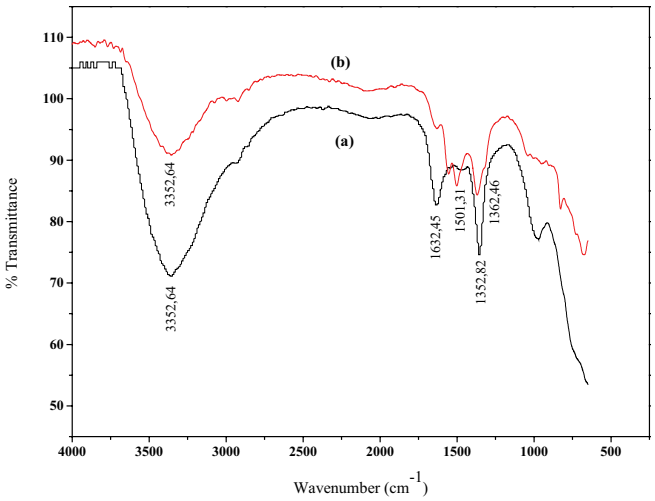

Fig. 3. Infrared spectra of synthesized (a) Ni–Fe and (b) Zn–Fe LDHs samples.

4.2. Study of Cochineal Red A removal with synthesized materials

4.2.1. Contact time and initial concentration effect on dye adsorption

In order to study the effect of initial dye concentration, the experiments were carried out at different initial concentrations ranging from 10 to 70 mg/L. The results are presented in Fig. 4. From the figure it is found that, the amount of CR dye adsorbed by synthesized materials increased with increasing the dye concentration and remained nearly constant after equilibrium time. The equilibrium time was 60 and 80 min for Ni–Fe and Zn–Fe LDHs respectively synthesized by co-precipitation at variable pH. This can be attributed to the fact that at the initial stage, the adsorption sites are more, and the CR dye can interact easily with the sites, so a higher adsorption rate is reached. Due to slower diffusion of solute into the interior of the adsorbent, a slow adsorption rate in later stage is observed [36].

The amount of dye adsorbed (q_e) from 6 to 43 mg/g as concentration was increased from 10 to 70 mg/L. The plots are single, smooth and continuous curves leading to saturation, suggesting the possible monolayer coverage to nitrate on the surface of the adsorbent [37].

4.2.2. Kinetic modelling

The sorption kinetic is an important aspect of processes for pollutant removal. To describe the mechanism for process sorption, the Lagergren first-order kinetic model and the pseudo-second-order model were applied which are mathematically expressed in Eqs. (3) and (4), respectively:

$$\frac{dq_t}{dt} = k_1\left(q_e - q_t\right) \tag{3}$$

$$\frac{dq_t}{dt} = k_2\left(q_e - q_t\right)^2 \tag{4}$$

where q_e and q_t are the amount of solute adsorbed per unit amount of adsorbent at equilibrium and at any time, t, respectively (mg/g), k_1 is the pseudo-first-order rate constant (min^{-1}), and k_2 is the pseudo-second-order rate constant (g/mg min).

After integration using the boundary conditions that at $t = 0$, $q_t = 0$, and that at $t = t$, $q_t = q_t$, the linear form of Eqs. (3) and (4) become respectively:

$$\ln\left(q_e - q_t\right) = \ln q_e - k_1 t \tag{5}$$

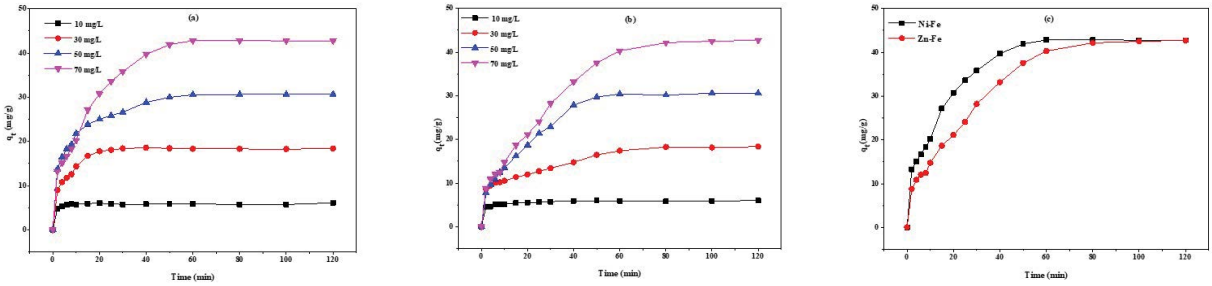

Fig. 4. Effect of time and initial concentration in the adsorption of CR on (a) Ni–Fe, (b) Zn–Fe and (c) on the two samples at 70 mg/L.

$$\frac{t}{q_t} = \frac{1}{k_2 q_e^2} + \frac{t}{q_t} \quad (6)$$

The experimental data were analyzed initially with first-order Lagergren model. The plot of $\ln(q_e - q_t)$ vs. t (Fig. 5) should give the linear relationship from which k_1 and q_e can be determined by the slope and intercept respectively [Eq. (5)]. The kinetic parameters for all experimental data are summarized in Table 1. The results showed that the theoretical calculated q_e (cal) value doesn't agree well with experimental q_e (exp) values at all concentrations studied with poor correlation coefficient. So, further the experimental data were fitted with second-order Lagergren model [Eq. (6)]. The equilibrium adsorption capacity, q_e (cal) and k_2 were determined from the slope and intercept of plot of t/q_t vs. t (Fig. 6) and are presented in Table 1. From the results, it is found that the theoretical q_e (cal) values much with experimental q_e (exp) values at all concentrations studied and a regression coefficient of above 0.99 shows that the adsorption system is a second-order, which implies that the adsorption of the Cochineal Red A dye onto synthesized materials is a chemical sorption rather than physical [38,39]. Similar results were reported in the literature with other adsorbents [40].

4.2.3. Sorption isotherm

The variation of the adsorbed dye quantity (q_e) according to the equilibrium concentration (C_e) is shown in Fig. 7. It follows that the equilibrium adsorption amount (q_e) increases with the increase of dye concentration (C_e). This finding is consistent with bibliographic data [30,38].

The results showed that there is no difference in the sorption ability of these materials. The nature and content of bi- and trivalent metal ions in LDH influence the adsorption. Goswamee et al. [41] have found that the adsorption capacity of $Cr_2O_7^{2-}$ in Mg–Al LDH with higher Al^{3+} content in the structure is higher than the product with lower Al^{3+} content. In the present study, the nature of bivalent metal ions influence the adsorption. As confirmed by XRD analysis, differences in the structural properties of each LDH were observed.

The adsorption capacity of the adsorbent has been tested using Freundlich and Temkin isotherms. These models have been widely used to describe the behavior of adsorbent–adsorbate couples. The obtained parameters for these models are summarized in Table 2.

The Freundlich isotherm is an empirical model relating to the adsorption intensity of the sorbent toward adsorbent. The isotherm is adopted to describe reversible adsorption and is not restricted to monolayer formation. The mathematical expression of the Freundlich model can be written as:

$$Q_e = K\, C_e^n \quad (7)$$

According to the Freundlich isotherm model, initially amount of adsorbed compounds increases rapidly;

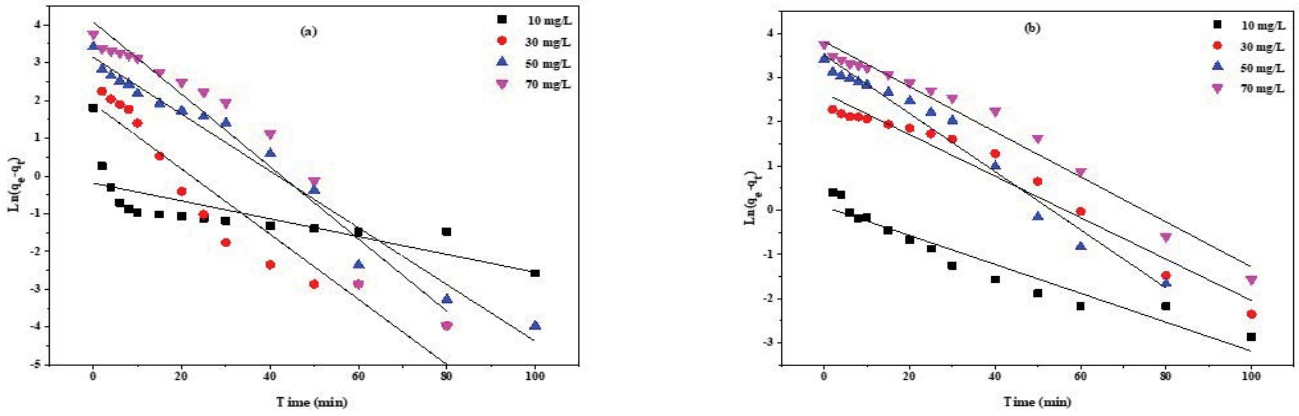

Fig. 5. Pseudo-first-order kinetic for adsorption of CR on (a) Ni–Fe and (b) Zn–Fe.

Table 1
Pseudo-first-order and pseudo-second-order kinetic parameters of Cochineal Red dye adsorption onto Ni–Fe and Zn–Fe LDHs at various initial dye concentration (T = 298 K)

Adsorbent	Initial dye concentration (mg/L)	q_e experimental (mg/g)	Pseudo-first-order			Pseudo-second-order		
			k_1 (min^{-1})	q_e calculated (mg/g)	R^2	k_2 (g/mg min)	q_e calculated (mg/g)	R^2
Ni–Fe	10	6.06	0.02361	0.82	0.5156	0.19104	6.01	0.9994
	30	18.39	0.08956	7.87	0.9008	0.02611	18.83	0.9990
	50	30.64	0.07522	23.14	0.9691	0.00791	31.79	0.9982
	70	42.77	0.09581	59.15	0.9396	0.00261	46.42	0.9917
Zn–Fe	10	6.01	0.03664	1.37	0.8176	0.12210	6.03	0.9997
	30	18.34	0.04753	14.64	0.9584	0.00690	19.24	0.9881
	50	30.55	0.06365	31.53	0.9029	0.00269	33.82	0.9850
	70	42.69	0.05098	45.33	0. 9743	0.00160	47.34	0.9817

Table 2
Temkin and Freundlich isotherm constants for the adsorption CR dye on Zn–Fe and Ni–Fe LDHs (T = 298 K)

Adsorbent	Temkin isotherm constants			Freundlich isotherm constants		
	A_T (mg/g min)	B_T (g/mg)	R^2	K_f	n	R^2
Ni–Fe	4.34	21.84	0.9955	29.27	0.86	0.9594
Zn–Fe	3.26	24.47	0.9970	24.82	0.77	0.9487

this increase slows down with increasing surface coverage. Eq. (11) can be linearized in logarithmic form and the Freundlich constants can be determined as follows [42]:

$$\log Q_e = \log K_f + \frac{1}{n}\log C_e \tag{8}$$

where C_e is the equilibrium concentration of adsorbate (mg/L), n is the amount of solute adsorbed, Q_e is the amount of dye adsorbed at equilibrium (mg/g) and K_f is Freundlich isotherm constant.

In testing the isotherm, the dye concentration used was 10 to 70 mg/L, the adsorption data are plotted as $\log Q_e$ vs. $\log C_e$ and should result in a straight line with slope "n" and intercept K_f. The intercept and the slope are indicators of adsorption capacity and adsorption intensity, respectively. The value of "n" in the range of 1 to 10 indicates favorable sorption. For Freundlich model, the n values were less than 1 (Table 2), indicating a low affinity between adsorbate and adsorbent.

The Temkin isotherm contains a factor that explicitly taking into the account of adsorbent–adsorbate interactions. By ignoring the extremely low and large value of concentrations, this model assumes that adsorption is characterized by a uniform distribution of binding energies between the molecules adsorbed and adsorbent. The linear form of this later is given by the equation:

$$Q_e = B \ln A_T + B \ln C_e \tag{9}$$

where A_T is Temkin isotherm equilibrium bending constant (L/g) and B is constant related to heat of sorption (J/mol).

The constants were determined from the slope and intercept of plot of the amount adsorbed Q_e vs. $\ln C_e$ (Fig. 8) and are presented in Table 2.

The constant B_T which is related to heat of sorption (J/mol) was estimated B_T = 24.47 and 21.84 J/mol for Zn–Fe and Ni–Fe respectively, indicates that the adsorption process is endothermic.

From the coefficients correlations values (R^2) obtained from the two sorption models, it was found that the dye adsorption on materials fitted the Temkin model better than the Freundlich model with high coefficient correlation, which may be due to the uniform distribution of binding energies between the molecules adsorbed and adsorbent [43].

4.2.4. Temperature effect

Fig. 9 shows the effect of the temperature on the removal of dye by the synthesized materials. It can be seen that the sorption capacity increases with increasing temperature. This is due to the increase in the mobility of pollutants in aqueous solution which facilitates the pollutant adsorption on actives sites [44].

The constants of thermodynamics $\Delta G°$, $\Delta H°$ and $\Delta S°$ are calculated using equation:

$$K_d = \frac{C_i - C_e}{C_e}\frac{V}{m} \tag{10}$$

$$\ln K_d = \frac{\Delta S°}{R} - \frac{\Delta H°}{RT} \tag{11}$$

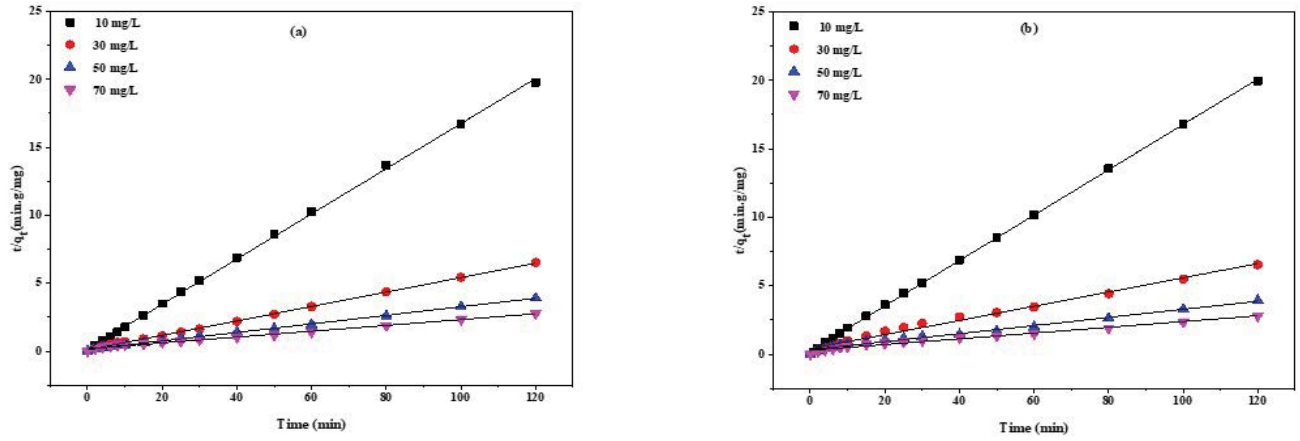

Fig. 6. Pseudo-second-order kinetic for adsorption of CR on (a) Ni–Fe and (b) Zn–Fe.

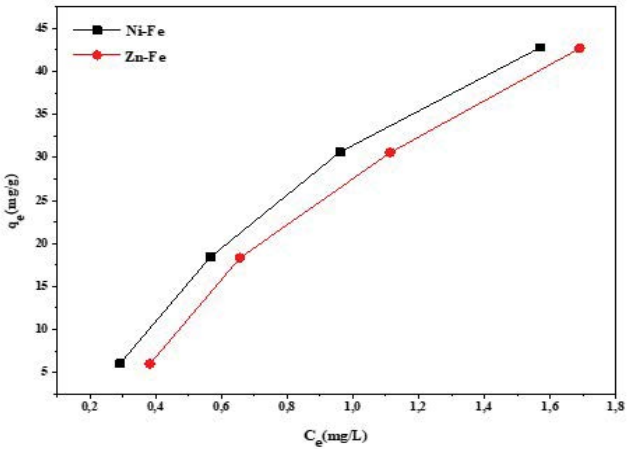

Fig. 7. CR sorption isotherms on the two samples.

where C_i is the initial concentration (mg/L), C_e is the equilibrium concentration (mg/L), V is the volume (mL) and m is the mass of adsorbent (g), R (8.314 J/mol K) is the ideal gas constant, and T (K) is the temperature in Kelvin. $\Delta H°$ is the enthalpy change and $\Delta S°$ is the entropy change in a given process. The values of enthalpy ($\Delta H°$) and entropy ($\Delta S°$) are calculated from the slope and y-intercept of the plot of $\ln K_d$ vs. $1/T$ by application the equations [45].

Free energy changes ($\Delta G°$) of adsorption are calculated from:

$$\Delta G° = \Delta H° - T\Delta S° \quad (12)$$

As given in Table 3, the values of $\Delta H°$ for Ni–Fe and Zn–Fe are determined as respectively 25.38 and 46.83 (kJ/mol).

The positives values of $\Delta H°$ confirm that the sorption process is endothermic in nature, which is different from the adsorption on alkali boiled Tilapia fish scales [8] where the adsorption of Cochineal Red A dye was exothermic. Also, the positives values of entropy may be due to the increase of randomness at the solid solution interface during the sorption. This implies some structural changes in sorbate and sorbent, which leads to an increase in the disorderness of the solid-solution system.

The negatives values of $\Delta G°$ indicate that adsorption is spontaneous. The values of $\Delta G°$ became more negatives with increasing temperature, showing that higher temperature facilitated the sorption of dye on these materials.

4.2.5. Adsorbent dose effect

The result of effect of sorbent dosage on the adsorption of dye into the synthesized materials are shown in Fig. 10.

It can be seen that the removal efficiency increases with increasing sorbent dosage until 40 and 80 mg of Ni–Fe and Zn–Fe LDHs respectively, and the removal efficiency remains almost unchanged after these doses. This may be explained by the good dispersion of materials particles on Cochineal Red solutions, which facilitates the dye adsorption on a large number of actives sites. In contrast, the adsorption capacity decreases very quickly with increasing sorbent dosage and also remains almost constant after a sorbent dosage of 40 and 80 mg for Ni–Fe and Zn–Fe respectively. The large amount of adsorbent reduces the unsaturation of adsorption sites and the number of sites per unit mass decreases, resulting in low adsorption for large amounts of adsorbent [3,44,46].

It can be observed that the quantity adsorbed is higher on Ni–Fe than on Zn–Fe material, and this from 20 to 60 mg of sorbent dosage. After this dose, the quantities of dye adsorbed on both materials are similar. This may be explained by the difference in the structure of materials as confirmed by XRD analysis and the content of trivalent metal ions in LDHs.

4.2.6. pH effect

The effect of solution pH on the removal of dye by the two synthesized materials is shown in Fig. 11. Based on the results, the dye adsorption on materials is practically constant at the pH range of 2–9.This indicates that LDH remove the anionic dye with the same efficiency in this range of pH values. When increasing the pH (10–11), a decrease was observed in the case of Zn–Fe, which has already been observed with

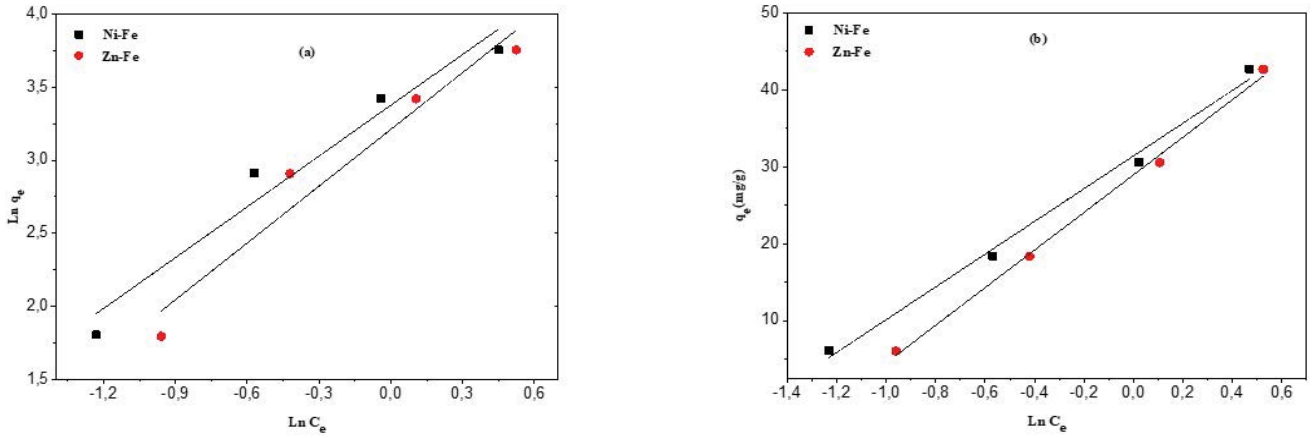

Fig. 8. Freundlich (a) and Temkin (b) plots for the sorption of CR by the two samples.

Table 3
Values of thermodynamic parameters for the adsorption of Cochineal Red dye onto Zn–Fe and Ni–Fe LDHs (C_i = 50 mg/L)

Adsorbent	Δ*H* (kJ/mol)	Δ*S* (J/mol K)	Δ*G* (kJ/mol)			
			298 K	308 K	318 K	328 K
Ni–Fe LDH	25.38	178.64	–53.21	–54.99	–56.78	–58.57
Zn–Fe LDH	46.83	229.94	–68.47	–70.77	–73.07	–75.37

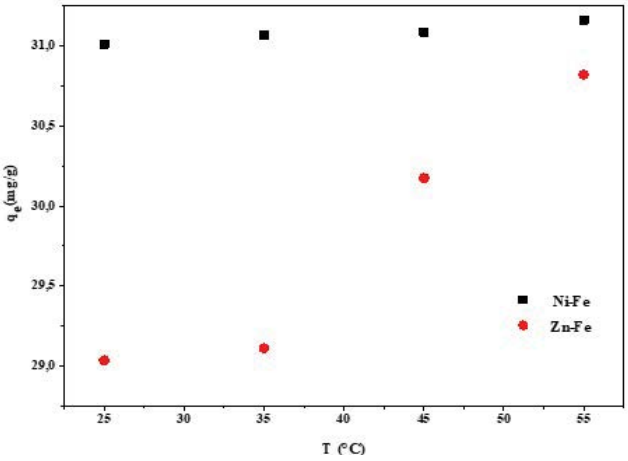

Fig. 9. Effect of temperature in the adsorption of CR on the two samples.

other adsorbents. This can be due to a decrease in the positive charge of the materials surface that can be neutralized by the excess of OH^- ions present in the medium [47,48].

4.2.7. Regeneration of the sorbents

The Cochineal Red dye adsorption efficiency of prepared materials was tested after two regeneration cycles. The first and second regenerations of Ni–Fe did not affect its dye adsorption capacity (19.8 g/mg). The same results were obtained for Zn–Fe (18.31 g/mg). This observation is very important for economic reasons and led to deduce that these adsorbents could be reused with the same efficiency.

5. Conclusion

The adsorption of Cochineal Red A on materials synthesized by a co-precipitation method at pH variable has been investigated.

Our results show that the kinetic and sorption data fitted well the second-order kinetic model and the Temkin model respectively with good values of determination coefficient. This indicates that the adsorption is characterized by a uniform distribution of binding energies between the molecules adsorbed and adsorbents.

The removal of Cochineal Red dye reaches its maximum of 98.44% and 96.86% after 60 min and 80 min for Ni–Fe and Zn–Fe respectively with the use of the optimum masses of 40 and 100 mg for these respective materials.

The thermodynamic study indicates that the dye sorption on synthesized materials is endothermic and spontaneous process.

The influence of different adsorption conditions as initial dye concentration, temperature, adsorbent dosage, and contact time and pH solution on dye removal was investigated for all materials.

The sorption was found to be a pH independent for Ni–Fe LDH material, whereas, sorption increases with increasing pH from 2 to 9 and decreases at high values of pH (from 9 to 11) for Zn–Fe LDH.

The sorbed amount depends on the nature and content of bi- and trivalent metal ions in LDH.

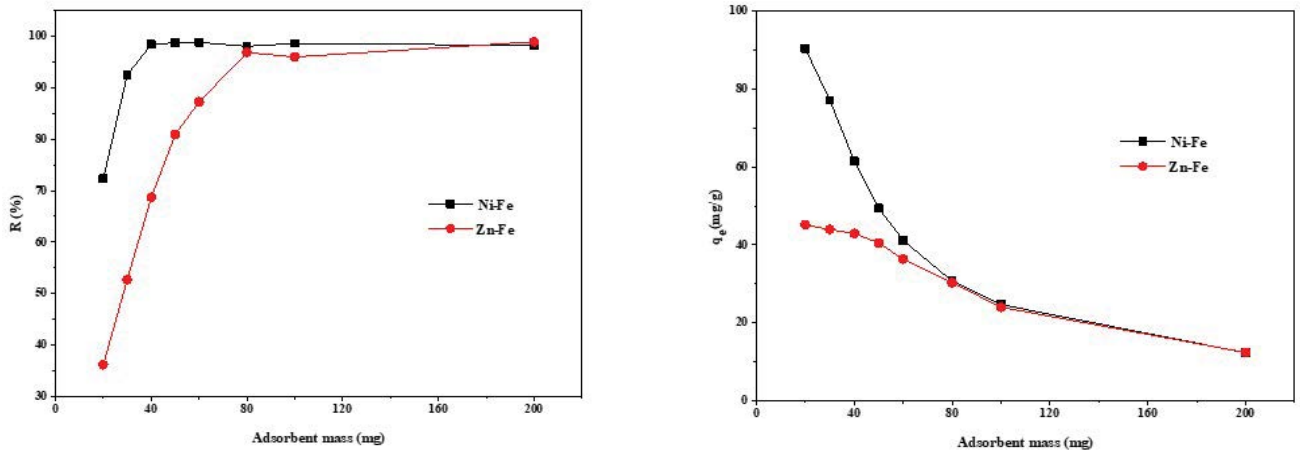

Fig. 10. Effect of adsorbent mass in the adsorption of CR on the two samples.

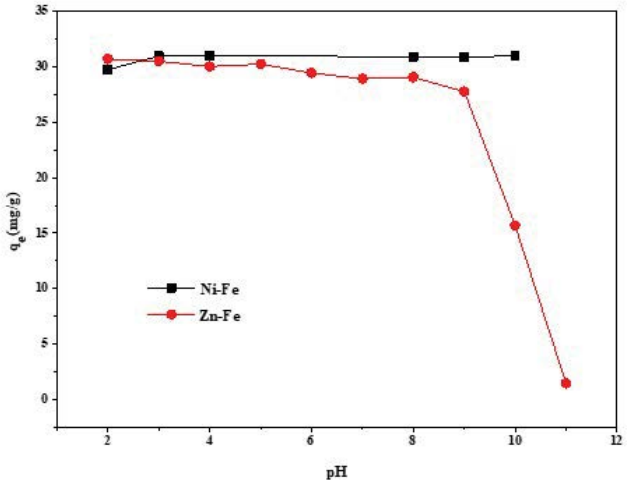

Fig. 11. Effect of solution pH in the adsorption of CR on the two samples.

The synthesized materials exhibited exceptional adsorption capacities indicating that these materials might be a potentially efficient materials for the removal of Cochineal Red dye from aqueous solutions.

References

[1] D.B. Jiang, C. Jing, Y. Yuan, L. Feng, X. Liu, F. Dong, B. Dong, Y.X. Zhang, 2D-2D growth of NiFe LDH nanoflakes on montmorillonite for cationic and anionic dye adsorption performance, J. Colloid Interface Sci., 540 (2019) 398–409.

[2] W. Stawiński, A. Węgrzyn, O. Freitas, L. Chmielarz, G. Mordarski, S. Figueiredo, Simultaneous removal of dyes and metal cations using an acid, acid-base and base modified vermiculite as a sustainable and recyclable adsorbent, Sci. Total Environ., 576 (2017) 398–408.

[3] N.B.H. Abdelkader, A. Bentouami, Z. Derriche, N. Bettahar, L.C. de Menorval, Synthesis and characterization of Mg–Fe layer double hydroxides and its application on adsorption of Orange G from aqueous solution, Chem. Eng. Sci., 169 (2011) 231–238.

[4] N.D. Mu'azu, N. Jarrah, T.S. Kazeem, M. Zubair, M. Al-Harthi, Bentonite-layered double hydroxide composite for enhanced aqueous adsorption of Eriochrome Black T, Appl. Clay Sci., 161 (2018) 23–34.

[5] K. Abdellaoui, I. Pavlovic, M. Bouhent, A. Benhamou, C. Barriga, A comparative study of the amaranth azo dye adsorption/desorption from aqueous solutions by layered double hydroxides, Appl. Clay Sci., 143 (2017) 142–150.

[6] Z. Li, L. Sellaoui, G. Luiz Dotto, A. Ben Lamine, A. Bonilla-Petriciolet, H. Hanafy, H. Belmabrouk, M. Schadeck Netto, A. Erto, Interpretation of the adsorption mechanism of Reactive Black 5 and Ponceau 4R dyes on chitosan/polyamide nanofibers via advanced statistical physics model, J. Mol. Liq., 285 (2019) 165–170.

[7] N.A. Salahuddin, H.A. EL-Daly, R.G. El Sharkawy, B.T. Nasr, Synthesis and efficacy of PPy/CS/GO nanocomposites for adsorption of ponceau 4R dye, Polymer, 146 (2018) 291–303.

[8] K. Zhu, X. Gong, D. He, B. Li, D. Ji, P. Li, Z. Peng, Y. Luo, Adsorption of Ponceau 4R from aqueous solutions using alkali boiled Tilapia fish scales, RSC Adv., 3 (2013) 25221–25230.

[9] K.-T. Chung, Azo dyes and human health: a review, J. Environ. Sci. Health., Part C Environ. Carcinog. Ecotoxicol. Rev., 34 (2016) 233–261.

[10] A. Lemoine, P. Tounian, Food-dye allergy: a pathology to be evoked sparingly, Rev. Fr. Allergol., 58 (2018) 506–5012.

[11] S. Tsuda, M. Murakami, N. Matsusaka, K. Kano, K. Taniguchi, Y.F. Sasaki, DNA damage induced by red food dyes orally administered to pregnant and male mice, Toxicol. Sci., 61 (2001) 92–99.

[12] R.W. Weber, M. Hoffman, D.A. Raine DA, H.S. Nelson, Incidence of bronchoconstriction due to aspirin, azo dyes, non-azo dyes, and preservatives in a population of perennial asthmatics, J. Allergy Clin. Immunol., 64 (1979) 32–37.

[13] X. Tao, D. Liu, W. Cong, L. Huang, Controllable synthesis of starch-modified ZnMgAl-LDHs for adsorption property improvement, Appl. Surf. Sci., 457 (2018) 572–579.

[14] M. Shamsayei, Y. Yamini, H. Asiabi, Fabrication of zwitterionic histidine/layered double hydroxide hybrid nanosheets for highly efficient and fast removal of anionic dyes, J. Colloid Interface Sci., 529 (2018) 255–264.

[15] M. Bouraada, M.S. Ouali, L.C. de Menorval, Dodecylsulfate and dodecybenzenesulfonate intercalated hydrotalcites as adsorbent materials for the removal of BBR acid dye from aqueous solutions, J. Saudi Chem. Soc., 20 (2016) 397–404.

[16] X. Yong, S. Raza, J. Deng, Y. Wu, Biomass ferulic acid-derived hollow polymer particles as selective adsorbent for anionic dye, React. Funct. Polym., 132 (2018) 9–18.

[17] D. Zhang, M.Y. Zhu, J.G. Yu, H.W. Meng, F.P. Jiao, Effective removal of brilliant green from aqueous solution with magnetic Fe_3O_4@SDBS@LDHs composites, Trans. Nonferrous Met. Soc. China, 27 (2017) 2673–2681.

[18] R. Kamaraj, D.J. Davidson, G. Sozhan, S. Vasudevan, Adsorption of 2,4-dichlorophenoxyacetic acid (2,4-D) from water by in situ generated metal hydroxides using sacrificial anodes, J. Taiwan Inst. Chem. Eng., 45 (2014) 2943–2949.
[19] R. Miandad, R. Kumar, M.A. Barakat, C. Basheer, A.S. Aburiazaiza, A.S. Nizami, M. Rehan, Untapped conversion of plastic waste char into carbon-metal LDOs for the adsorption of Congo red, J. Colloid Interface Sci., 511 (2018) 402–410.
[20] L. El Gaini, M. Lakraimi, E. Sebbar, A. Meghea, M. Bakasse, Removal of indigo carmine dye from water to Mg–Al–CO_3-calcined layered double hydroxides, J. Hazard. Mater., 161 (2009) 627–632.
[21] Z. Yang, F. Wang, C. Zhang, G. Zeng, X. Tan, Z. Yu, Y. Zhong, H. Wang, F. Cui, Utilization of LDH-based materials as potential adsorbents and photocatalysts for the decontamination of dyes wastewater: a review, RSC Adv., 6 (2016) 79415–79436.
[22] Y.F. Tao, W.G. Lin, L. Gao, J. Yang, J.H. Zhu, Low-cost and effective phenol and basic dyes trapper derived from the porous silica coated with hydrotalcite gel, J. Colloid Interface Sci., 358 (2011) 554–561.
[23] F.P. Jiao, Z.D. Fu, L. Shuai, X.Q. Chen, Removal of phenylalanine from water with calcined CuZnAl-CO_3 layered double hydroxides, Trans. Nonferrous Met. Soc. China, 22 (2012) 476–482.
[24] M.A. Djebbi, M. Braiek, P. Namour, A.B.H. Amara, N. Jaffrezic-Renault, Layered double hydroxide materials coated carbon electrode: new challenge to future electrochemical power devices, Appl. Surf. Sci., 386 (2016) 352–363.
[25] Y.X. Zhang, X.D. Hao, M. Kuang, H. Zhao, Z.Q. Wen, Preparation, characterisation and dye adsorption of Au nanoparticles /ZnAl layered double oxides nanocomposites, Appl. Surf. Sci., 283 (2013) 505–512.
[26] R. Zhang, Y. Ai, Z. Lu, Application of multifunctional layered double hydroxides for removing environmental pollutants: recent experimental and theoretical progress, J. Environ. Chem. Eng., 8 (2020) 103908, doi: 10.1016/j.jece.2020.103908.
[27] D.B. Jiang, C. Jing, Y. Yuan, L. Feng, X. Liu, F. Dong, B. Dong, Y.X. Zhang, 2D-2D growth of NiFe LDH nanoflakes on montmorillonite for cationic and anionic dye adsorption performance, J. Colloid Interface Sci., 540 (2019) 398–409.
[28] F.P. de Sá, B.N. Cunha, L.M. Nunes, Effect of pH on the adsorption of Sunset Yellow FCF food dye into a layered double hydroxide (CaAl-LDH-NO_3), Chem. Eng. J., 215 (2013) 122–127.
[29] W. Chouchene, U.R. de Catalyse, Humid air plasma treatment of birnessite surface: application to the removal of Cochineal Red, J. Mater. Sci. Appl., 6 (2015) 1014–1021.
[30] M. Bouraada, M. Lafjah, M.S. Ouali, L.C. de Menorval, Basic dye removal from aqueous solutions by dodecylsulfate- and dodecyl benzene sulfonate-intercalated hydrotalcite, J. Hazard. Mater., 153 (2008) 911–918.
[31] M. Zubair, N. Jarrah, M.S. Manzar, M. Al-Harthi, M. Daud, N.D. Mu'azu, S.A. Haladu, Adsorption of Eriochrome black T from aqueous phase on MgAl-, CoAl- and NiFe-calcined layered double hydroxides: kinetic, equilibrium and thermodynamic studies, J. Mol. Liq., 230 (2017) 344–352.
[32] J.T. Kloprogge, L. Hickey, R.L. Frost, The effects of synthesis pH and hydrothermal treatment on the formation of zinc aluminum hydrotalcites, J. Solid State Chem., 177 (2004) 4047–4057.
[33] M.A. Djebbi, Layered Doubles Hydroxides at the Heart of Biotechnology: Evaluation of Medical and Environmental Applications, Ph.D. Thesis, University of Lyon, 2017.
[34] F.M. Labajos, V. Rives, M.A. Ulibarri, Effect of hydrothermal and thermal treatments on the physicochemical properties of Mg-Al hydrotalcite-like materials, J. Mater. Sci., 27 (1992) 1546–1552.
[35] H. Zaghouane-Boudiaf, M. Boutahala, C. Tiar, L. Arab, F. Garin, Treatment of 2,4,5-trichlorophenol by MgAl–SDBS organo-layered double hydroxides: kinetic and equilibrium studies, Chem. Eng. J., 173 (2011) 36–41.
[36] M. Islam, R. Patel, Nitrate sorption by thermally activated Mg/Al chloride hydrotalcite-like compound, J. Hazard. Mater., 169 (2009) 524–531.
[37] R. Kamaraj, A. Pandiarajan, S. Jayakiruba, Mu. Naushad, S. Vasudevan, Kinetics, thermodynamics and isotherm modeling for removal of nitrate from liquids by facile one-pot electro synthesized nano zinc hydroxide, J. Mol. Liq., 215 (2016) 204–211.
[38] C. Jiang, B. Fu, H. Cai, T. Cai, Efficient adsorptive removal of Congo red from aqueous solution by synthesized zeolitic imidazolate framework-8, Chem. Speciation Bioavailability, 28 (2016) 199–208.
[39] P. Ganesan, J. Lakshmi, G. Sozhan, S. Vasudevan, Removal of manganese from water by electrocoagulation: adsorption, kinetics and thermodynamic studies, Can. J. Chem. Eng., 91 (2013), doi: 10.1002/cjce.21709.
[40] M. Borysiak, E. Gabruś, Adsorptive removal of Cochineal Red A dye from aqueous solutions using yeast, Chem. Eng. Process., 41 (2020) 105–117.
[41] R.L. Goswamee, P. Sengupta, K.G. Bhattacharyya, D.K. Dutta, Adsorption of Cr(VI) in layered double hydroxides, Appl. Clay Sci., 13 (1998) 21–34.
[42] S. Vasudevan, J. Lakshmi, G. Sozhan, Electrocoagulation studies on the removal of copper from water using mild steel electrode, Water Environ. Res., 84 (2012) 209–219.
[43] A. Guzmán-Vargas, E. Lima, G.A. Uriostegui-Ortega, M.A. Oliver-Tolentino, E.E. Rodríguez, Adsorption and subsequent partial photodegradation of methyl violet 2B on Cu/Al layered double hydroxides, Appl. Surf. Sci., 363 (2016) 372–380.
[44] M. Zubair, M. Daudb, G. McKay, F. Shehzad, M.A. Al-Harthi, Recent progress in layered double hydroxides (LDH)-containing hybrids as adsorbents for water remediation, Appl. Clay Sci., 143 (2017) 279–292.
[45] N. Caliskan, A.R. Kul, S. Alkan, E.G. Sogut, İ. Alacabey, Adsorption of zinc(II) on diatomite and manganese-oxide-modified diatomite: a kinetic and equilibrium study, J. Hazard. Mater., 193 (2011) 27–36.
[46] H. Zaghouane-Boudiaf, M. Boutahala, L. Arab, Removal of methyl orange from aqueous solution by uncalcined and calcined MgNiAl layered double hydroxides (LDHs), Chem. Eng. J., 187 (2012)142–149.
[47] B.K. Nandi, A. Goswami, M.K. Purkait, Adsorption characteristics of brilliant green dye on kaolin, J. Hazard. Mater., 161 (2009) 387–395.
[48] R.M.M. dos Santos, R.G.L. Gonçalves, V.R.L. Constantino, L.M. da Costa, L.H.M. da Silva, J. Tronto, F.G. Pinto, Removal of Acid Green 68:1 from aqueous solutions by calcined and uncalcined layered double hydroxides, Appl. Clay Sci., 80 (2013) 189–195.